HHS Public Access

Author manuscript

Neurobiol Aging. Author manuscript; available in PMC 2018 February 01.

Published in final edited form as:

Neurobiol Aging. 2017 February ; 50: 96–106. doi:10.1016/j.neurobiolaging.2016.11.002.

White matter damage and glymphatic dysfunction in a model of vascular dementia in rats with no prior vascular pathologies

Poornima Venkat, PhD[a,b], **Michael Chopp, PhD**[a,b], **Alex Zacharek, MS**[a], **Chengcheng Cui, MD**[a], **Li Zhang, MD**[a], **Qingjiang Li, MS**[a], **Mei Lu, PhD**[d], **Talan Zhang, MS**[e], **Amy Liu**[a], and **Jieli Chen, MD**[a,c,#]

[a] Neurology Research, Henry Ford Hospital, Detroit, MI, USA

[b] Department of Physics, Oakland University, Rochester, MI, USA

[c] Department of Geriatrics, Tianjin Geriatrics Institute, Tianjin Medical University General Hospital, Tianjin, China

[d] Biostatistics and Research Epidemiology, Henry Ford Hospital, Detroit, MI, USA

[e] Public Health Sciences, Henry Ford Hospital, Detroit, MI, USA

Abstract

We investigated cognitive function, axonal/white matter (WM) changes and glymphatic function of vascular dementia (VaD) using a multiple microinfarction (MMI) model in retired breeder (RB) rats. The MMI model induces significant ($p<0.05$) cognitive decline that worsens with age starting at 2 weeks, which persists until at least 6 weeks after MMI. RB rats subjected to MMI exhibit significant axonal/WM damage identified by decreased myelin thickness, oligodendrocyte progenitor cell numbers, axon density, synaptic protein expression in the cortex and striatum, cortical neuronal branching, and dendritic spine density in the cortex and hippocampus compared with age matched controls. MMI evokes significant dilation of perivascular spaces as well as water channel dysfunction indicated by decreased Aquaporin-4 (AQP-4) expression around blood vessels. MMI induced glymphatic dysfunction with delayed cerebrospinal fluid (CSF) penetration into the brain parenchyma via paravascular pathways as well as delayed waste clearance from the

[#] Corresponding author: Jieli Chen, MD, Senior Staff Investigator, Henry Ford Hospital, Neurology Research, E&R Building, 3091, Detroit, MI, 48202, Phone: (313) 916-1991; Fax: (313) 916-1318. jieli@neuro.hfh.edu.
pvenkat3@hfhs.org, mchopp1@hfhs.org, alexz@neuro.hfh.edu, cheng868823@163.com, lzhang@neuro.hfh.edu, qli1@hfhs.org, mlu1@hfhs.org, tzhang1@hfhs.org, from.amyliu@gmail.com

Disclosures: None

1. All authors disclose that there are no conflicts of interest including any financial, personal or other relationships with other people or organizations within three years of beginning the work submitted that could inappropriately influence (bias) their work.
2. We verify that there are none of the author's institution has contracts relating to this research through which it or any other organization may stand to gain financially now or in the future.
4. All authors verify that the data contained in the manuscript being submitted have not been previously published, have not been submitted elsewhere and will not be submitted elsewhere while under consideration at Neurobiology of Aging.
5. All authors have reviewed the contents of the manuscript being submitted, approve of its contents and validate the accuracy of the data.

brain. The MMI model in RB rats decreases AQP-4 and induces glymphatic dysfunction which may play an important role in MMI induced axonal/WM damage and cognitive deficits.

Keywords

vascular dementia; aquaporin 4; white matter; glymphatic system; multiple microinfarction

1. Introduction

Vascular Dementia (VaD) is a progressive disease that affects cognition and memory. VaD accounts for nearly 20% of all dementia patients and is the second leading form of dementia after Alzheimer's disease (Plassman, et al., 2007). VaD, also known as multi infarct dementia, is caused by a decrease in blood flow to the brain and is typically associated with a cerebrovascular accident such as a stroke or series of minor strokes. In multi infarct dementia, emboli composed of cholesterol or of fragments of atheromatous plaques or thrombus, typically lodge in and block small arteries and induce multiple micro-infarcts in the cortex and striatum (Venkat, et al., 2015). Atheroemboli are the most common type of emboli encountered in VaD. The multiple microinfarction (MMI) model using cholesterol crystals closely mimics atheroembolization. MMI in rodents induces cognitive dysfunction and pathological features similar to human VaD, and induces delayed demyelination, hippocampal damage, blood brain barrier (BBB) damage, and inflammation (Laloux and Brucher, 1991,Rapp, et al., 2008b,Steiner, et al., 1980,Venkat, et al., 2015).

In this study, we employ a previously described and accepted MMI model using cholesterol crystals to induce VaD (Rapp, et al., 2008a,Rapp, et al., 2008b,Wang, et al., 2012) and investigate for the first time selective pathophysiological events driving white matter (WM) damage and cognitive deficits.

Aquaporins are integral membrane pore proteins that transport and regulate water movement in the brain. AQP-4 is predominantly present in astrocytic endfeet near capillaries and in cells lining the ventricles which are key sites for water movement between the cellular, vascular, and ventricular compartments (Papadopoulos, et al., 2002). The glymphatic system is an effective waste clearance pathway that removes metabolic wastes and neurotoxins from the brain along paravascular channels (Jessen, et al., 2015). The paravascular space is filled with cerebrospinal fluid (CSF) and CSF flows parallel to blood flow (Jessen, et al., 2015). Around penetrating vessels, paravascular spaces take the form of Virchow-Robin spaces, also called perivascular space. While the perivascular spaces terminate within the brain parenchyma, paravascular CSF can continue traveling along the basement membranes surrounding arterial vascular smooth muscle, to reach the basal lamina surrounding brain capillaries. CSF movement along these paravascular pathways is rapid, and arterial pulsation been implicated as a major driving force for paravascular fluid movement (Rennels, et al., 1985). AQP-4 mediated water channels facilitate extensive movement of CSF into the brain, CSF-ISF (interstitial fluid) exchange and interstitial solute clearance, and post injury edema formation and resolution (Badaut, et al., 2011,J. J. Iliff, et al., 2014). Disruption of the AQP-4 mediated water channel and failure of the glymphatic system burdens the brain with

accumulating waste, and has been reported in aging as well as several neurological diseases such as Alzheimer's disease, stroke and diabetes (Jessen, et al., 2015,Jiang, et al., 2016). However, whether glymphatic dysfunction and associated decreased AQP-4 expression influences vascular dementia has not been investigated.

In this study, we investigated cognitive deficits induced by an MMI based VaD model in young and retired breeder (RB) male rats, and its underlying disease mechanisms such as axonal/WM damage, synaptic disruption, as well as water channel and glymphatic system dysfunction.

2. Materials and Methods

All experiments were conducted in accordance with the standards and procedures of the American Council on Animal Care and Institutional Animal Care and Use Committee of Henry Ford Health System.

2.1. Cholesterol crystals preparation and MMI model

In this study we employ a previously described MMI model. Cholesterol crystals were freshly prepared (Rapp, et al., 2008a,Rapp, et al., 2008b,Wang, et al., 2012) (summarized in supplementary Figure 1), and were filtered using 100μm cell strainer with filtrate passed through a 70μm cell strainer to collect residual crystals of size 70-100μm. The crystals were counted on a hemocytometer and diluted to yield a final concentration of 500±100 crystals/ 300μl saline/per rat.

Male young adult (young, 3-4 months) and retired breeder (RB, 6-8 months) Wistar rats were subjected to the MMI model, as previously described (Rapp, et al., 2008a,Rapp, et al., 2008b,Wang, et al., 2012). Briefly, rats were anesthetized with 2% isoflurane in a jar for pre-anesthetic, and spontaneously respired with 1.5% isoflurane in 2:1 N_2O:O_2 mixture using a facemask connected and regulated with a modified FLUOTEC 3 Vaporizer (Fraser Harlake, Orchard Park, NY). Rectal temperature was maintained at 37°C throughout the surgical procedure using a feedback regulated water heating system. A midline neck incision was made and the right CCA (common carotid artery), ECA (external carotid artery), and ICA (internal carotid artery) were exposed under an operating microscope. Carefully avoiding the vagus nerve, the CCA and ICA were temporarily clamped using microsurgical clips and a 5-0 silk suture was tied loosely at the origin of the ECA and ligated at the distal end of the ECA. A 1ml syringe connected to a PE-50 tube, with its tip tapered by heating near a flame was inserted into the ECA through a small incision made with micro scissors. The tube was gently advanced from the ECA into the lumen of the ICA and the microsurgical clip was repositioned to only block the CCA. The freshly prepared cholesterol crystals were slowly injected into the ICA over a minute. The tube was gently removed, ECA ligated, microsurgical clips removed and the neck incision was closed. The animals were moved to their home cages to awaken. A battery of cognitive tests was performed, and rats were sacrificed at 4 weeks after MMI. Additional sets of RB rats were prepared and sacrificed at the 2^{nd}, 4^{th} and 6^{th} week after MMI to assess VaD progression (N=6/group). Naïve age matched controls were employed throughout this study (N=6/group).

2.2. Function tests

An investigator blinded to the experimental groups performed a battery of neurological function and cognitive tests.

Neurological function tests: Modified neurological severity score (mNSS) is a composite of motor, sensory, balance and reflex tests with scores between 0-18 (normal score 0; maximal deficit score 18) (Chen, et al., 2001). mNSS was performed at days 1, 7, 14, 21 and 28 after MMI.

Cognitive tests: The novel object recognition test (Stuart, et al., 2013) with a retention delay of 4 hours was carried out to assess visual learning and short term memory based on animal bias to explore new objects. The odor test (Spinetta, et al., 2008) that evaluates olfactory learning and memory based on an animal's preference for new smells was conducted with a retention delay of 24 hours and used to test long term memory. An open field evaluation (Brown, et al., 1999) was performed for 5 minutes to assess locomotor activity and anxiety-like behavior. The Morris water maze (MWM) test (Darwish, et al., 2012) was used to evaluate spatial and visual learning and memory with averse motivation to assess hippocampal memory deficits.

2.3. Histological and Immunohistochemical assessment

The animals were sacrificed and transcardially perfused with 0.9% saline. Brains were immediately removed and fixed in 4% paraformaldehyde. Seven coronal sections of tissue were processed and stained with H&E for identification of infarctions. Brain coronal tissue sections were prepared and antibody against NG2 (oligodendrocyte progenitor cell (OPC) marker, Chemicon (EMD Millipore), Billerica, MA, 1:400), synaptophysin (synaptic protein, Abcam, Cambridge, MA, 1:400), FITC (Fluorescein isothiocyanate) labeled AQP-4 (Aquaporin-4, EMD Millipore, Billerica, MA, 1:1500) were used. BS (Bielschowsky silver, axon marker), LFB (Luxol fast blue, myelin marker) and Golgi staining (FD NeuroTechnologies, Columbia, MD, Rapid Golgi stain kit, and manufacturer's protocol was used) were used. Control experiments consisted of staining brain coronal tissue sections as outlined above, but non-immune serum was substituted for the primary antibody. In addition, internal positive controls were also employed.

2.4. Quantification analysis

Slides from each brain containing 4 fields of view of ipsilateral striatum, cortex or corpus callosum were digitized under a 20× objective (Olympus BX40) using a 3-CCD color video camera with an MCID image analysis system as indicated in Figure 1A close to regions of expected damage. In the WM bundles of the striatum and/or corpus callosum, using MCID image analysis the numbers of immunoreactive cells were counted or positive stained areas were measured (densitometry function) with a density threshold above unstained set uniformly for all groups (Chen, et al., 2016,Yan, et al., 2015,Yan, et al., 2014). All striatal vessels with diameter >10μm were selected without bias and perivascular space was quantified as previously described (Ampawong, et al., 2011). To evaluate water channel dysfunction, AQP-4 positive areas were measured around these blood vessels under 40× magnification. Neurite branching was counted under a 40× objective and 10 intact neurons

from the layer III of cortex were chosen and primary and secondary branching counted. For evaluation of spine density, 10 neurons from each brain sample in layer III of cortex and CA3 region of hippocampus were digitized under an oil immersion 100× objective, and ten stretches of secondary dendrites of at least 10μm in length were analyzed.

2.5. Electron microscopy (EM)

To further confirm and analyze axonal/WM damage, EM was employed in retired breeder MMI rats (n=4/group). For analysis of myelin thickness, number of demyelinated axons and G ratio (ratio of axon internal to external diameter) in the corpus callosum, a thin section of corpus callosum was prepared for EM analysis. Samples from each brain containing 8 fields of view of corpus callosum were digitized under 7100× magnification and analyzed using an MCID image analysis system.

2.6. FITC-dextran perfusion

To visualize cerebral microinfarctions after MMI in RB rats; FITC-dextran (FD2000S, Sigma; 50mg/rat in 2ml PBS) was injected intravenously at 1 day after MMI; 5 minutes before sacrifice (Prakash, et al., 2013,Zhang, et al., 2000). Brain tissues were fixed by 4% paraformaldehyde for 48 hours then were processed to acquire adjacent 100μm thick coronal sections using a vibratome and imaged using a laser scanning confocal microscopy.

2.7. Glymphatic function

To assess glymphatic function, an additional set of RB control and MMI rats were prepared (n=18/group). At 2 weeks after MMI and in control rats, 50μl of 1% (diluted in artificial CSF) Texas Red conjugated dextran (MW: 3 kD, Invitrogen) and FITC conjugated dextran (MW: 500 kD, Invitrogen) at 1:1 ratio were injected into the cisterna magna over 30 minutes using a syringe pump. Rats (6/group/time point) were sacrificed at 30 minutes, 3 hours, and 6 hours from the start of infusion and were perfusion fixed. Vibratome sections (80μm thick) were cut to analyze tracer movement along paravascular pathways. The experiment and measurements followed previously described procedures (Yang, et al., 2013). To analyze the time sequenced ex-vivo fluorescence imaging of coronal sections, laser scanning confocal microscopy was used.

2.8. Statistical Analysis

Data were evaluated for normality; ranked data were used for analysis when data were not normally distributed. Generalized Linear Model was performed to test MMI effect, age effect, and age by MMI interaction on Water Maze, cognitive test and mNSS at each day. Statistical significance was detected at $p<0.05$. The Global test using Generalize Estimating Equations was used to test MMI effect on immunostaining. The analysis began with testing the overall MMI effect, followed by pair-wise MMI effect for each test. Any subgroup analysis was considered exploratory if the overall MMI effect was not observed. The Global test was performed using PROC GENMOD in SAS 9.4. The CONTRAST statement in SAS was used to estimate the mean difference between the MMI groups and control based on the ranked data. All data are presented as mean ± SE. Pearson correlation coefficient was calculated. Statistical significance was detected at $p<0.05$.

3. Results

3.1. MMI in RB rats induces WM damage in the corpus callosum and striatal WM bundles

Figure 1A shows that MMI in RB rats induces significant WM rarefaction in the corpus callosum at 2 weeks after MMI. MMI model in young adult rats did not significantly induce WM damage compared to control rats (supplementary figure 2). MMI in RB rats induces microinfarcts in the striatum at 1 day after MMI indicated by FITC-dextran perfusion (supplementary figure 3). The data indicate that the MMI model in RB rats induced prominent VaD and was therefore subsequently used for immunostaining, EM, Golgi staining and glymphatic study.

To test the effect of MMI on axonal/WM damage, BS and LFB staining were performed. Figures 1B-D indicate that MMI in RB rats induces significant axonal damage and myelin loss in the corpus callosum and striatal WM bundles which persist until at least 6 weeks after MMI.

To further confirm and analyze axonal/WM damage, electron microscopy was employed. Figure 2 shows that MMI significantly ($p<0.05$) decreases myelin thickness, increases number of demyelinated axons and the G ratio in the corpus callosum of RB rats compared to RB control rats. These data indicate that the MMI induces WM damage in RB rats.

There was significant age by MMI interaction on LFB (Corpus Callosum: $p=0.0209$ and Striatum: $p=0.0053$) and BS (Striatum: $p=0.0369$). There was no significant age by MMI interaction on BS (Corpus Callosum ($p=0.4569$)) and AQP-4 ($p=0.1293$); but after removing the interaction term, significant MMI effect was detected (p value<0.0001). Overall, there were significant difference between Young and RB groups ($P<0.05$; worse in RB group).

3.2. MMI model induces VaD and cognitive deficits which worsen with increasing age

Figure 3 indicates that, MMI induces significant short term (novel object recognition test) and long term (odor test) memory loss, induces anxiety-like behavior and decreases exploratory activity (open field test) compared to age matched controls. Cognitive dysfunction post MMI is worse in RB rats compared to young adult rats. In the water maze test, young adult rats do not show spatial learning and memory deficits after MMI. RB rats after MMI suffer significant spatial learning and memory deficits compared to control RB rats. While there weren't significant differences between young and RB controls, MMI in RB rats induces significantly worse spatial learning and memory compared to MMI in young rats (supplementary figure 4). There was significant age by MMI interaction in novel object recognition test which was worse in MMI group and MMI had significant effect in different age groups. In odor test, open field test and water maze test, there was no significant age by MMI interaction; but after removing the interaction term, significant MMI effect was detected ($p<0.05$), and cognition was worse in MMI group. There was no significant difference between Young and RB groups in odor test but there were significant difference between Young and RB groups ($p<0.05$; worse in RB group) in open field and water maze tests.

Since motor deficits may influence cognitive testing, neurological deficits were assessed weekly after MMI. Compared to young adult rats, MMI in RB rats induced higher neurological deficits; however, these deficits were slight and significantly improved by 21-28 days after MMI. There were no significant differences by day 28 after MMI between young and RB rats subject to MMI. In addition, overall scores at 21-28 days after MMI were not severe to influence the results of cognitive evaluation (supplementary figure 5).

3.3. MMI in RB rats decreases the number of OPCs in the corpus callosum and striatum

OPCs are needed for myelination. OPCs contribute to myelin maintenance and repair by generating new oligodendrocytes as a source of remyelination and repair after brain injury. To further test the myelin damage, OPCs were identified using NG2 staining. Figure 4A indicates that MMI in RB rats significantly decreases the number of OPCs in the corpus callosum as well as striatum. This significant decrease persists until at least 6 weeks after MMI compared to RB control rats.

3.4. MMI in RB rats decreases synaptic plasticity

To test the effect of MMI on synaptic protein expression, synaptophysin expression was measured in RB rats. Figure 4B shows that MMI significantly decreased synaptophysin expression in the cortex and striatum.

To test the effect of MMI on neuronal branching and spine density, Golgi silver staining was used. Figure 5 shows that MMI in RB rats significantly decreases primary neuronal branching in the layer III of cortex as well as decreases dendritic spine density in the cortex and hippocampus CA3 region compared to RB control rats.

3.5. MMI in RB rats induces perivascular space dilation, water channel dysfunction and glymphatic system dysfunction

Figure 6 shows that MMI significantly increases perivascular spaces around vessels in the striatum compared to normal control RB rats. Since AQP-4 mediated water channel regulation plays an important role in the regulation of interstitial fluid and solute clearance, AQP-4 expression around blood vessels was measured. Figure 6B shows that MMI in RB rats significantly decreases AQP-4 expression around blood vessels in the brain and this water channel dysfunction persists until at least 6 weeks after MMI. AQP-4 loss around blood vessels after MMI significantly correlates with cognitive loss (odor: $R=0.614$, $p=0.04$; NOR: $R=0.776$, $p=0.005$; MWM: $R=-0.677$, $p=0.02$). MMI model in young adult rats did not significantly induce water channel dysfunction compared to control rats (supplementary figure 2).

MMI also induces functional impairment of the glymphatic system as indicated in Figure 6C-D. The results of the time sequenced ex-vivo fluorescence imaging of rat brain coronal sections indicates that there is impairment in CSF penetration into the brain parenchyma via paravascular pathways. Compared to control rats, CSF penetration in MMI rats was delayed at early time points (30 minutes) both along paravascular pathways as well as along the pial surface. Additionally, while in control rats a trend of clearance of dyes is observed, MMI rat

brain sections retain high levels of fluorescence at 6 hours after dye injection. These data indicate that MMI model induces glymphatic dysfunction.

4. Discussion

In this study, we have demonstrated that an MMI model using cholesterol crystals age-dependently induces VaD, with RB rats exhibiting more evident VaD than young rats. The MMI model in RB rats induces cognitive deficits such as short and long term memory loss, spatial learning and memory deficits as well as anxiety-like behavior which can persist until at least 6 weeks after MMI. MMI in RB rats induces significant WM rarefaction (early), decreases myelin thickness and OPC and OL numbers, increases axonal loss, decreases synaptic protein expression in the cortex and striatum, and decreases cortical neuronal branching and dendritic spine density in the cortex and hippocampus. MMI induces significant dilation of perivascular spaces around arteries. MMI also induces glymphatic pathway dysfunction with delayed CSF penetration and water channel dysfunction indicated by a decrease in AQP-4 expression around blood vessels. In addition, this AQP-4 loss around vessel significantly correlates with cognitive deficits.

4.1 MMI model age dependently regulates cognitive deficits

Increasing age has been reported as a strong risk factor for dementia. Brain tissue microstructure assessed with neurite orientation dispersion and density imaging was significantly decreased with age (Merluzzi, et al., 2016). WM damage related cognitive and affective functions worsen with age in AD and Parkinson's disease patients (Tokuchi, et al., 2016). Consistent with these findings, in our study we found that middle aged rats induced worse WM damage and cognitive functional deficits compared to young adult MMI rats. The severity of WM damage after MMI may be related to poorer cognitive outcome after MMI in middle aged rats compared to young adult MMI rats.

4.2. MMI model induces WM damage in RB rats

Several clinical VaD studies in humans have reported extensive WM damage in the periventricular region (Erkinjuntti, et al., 1996,Tanabe, et al., 1999). Compared to patients with AD, VaD patients suffer severe WM damage, arteriosclerosis-like changes, WM vacuolization and demyelination particularly in the periventricular region (Erkinjuntti, et al., 1996). Also, the periventricular frontal lobe and caudate head suffers from the highest density and frequency of lacunar infarction (Ishii, et al., 1986). This periventricular WM damage which disrupts the neuronal connections to the frontal lobe may be central to VaD induced cognitive deficits (Sultzer, et al., 1995). In RB MMI rats, we have observed WM rarefaction early after MMI as well as loss of axon density and demyelination in the corpus callosum and WM bundles in the striatum. Using EM, we found a significant reduction in myelin thickness, increased number of unmyelinated axons and increased G ratio in the corpus callosum of RB MMI rats compared to age-matched control rats. Myelin is essentially an insulation wrapped around the axons to accelerate conduction of nerve impulses. Along with controlling the speed of impulse conduction through axons, myelin also maintains the coordination of impulse transmission between distant cortical regions which is vital for cognition and learning (Fields, 2008). Remyelination involves

oligodendrocytes which originate from OPCs and produce new myelin sheaths on demyelinated axons. During the recovery phase of some neurological diseases such as stroke, there is an increase in OPC numbers and some of the OPCs become mature myelinating oligodendrocytes in the ischemic penumbra (Zhang, et al., 2013). A transient increase of NG2 positive OPCs in demyelinating lesions has been reported in a chronic cerebral ischemia model of VaD at 4 weeks after VaD onset that did not persist until 6, 8, or 12 weeks (Chida, et al., 2011). However, in WM diseases like multiple sclerosis and VaD, remyelination failure during disease progression eventually occurs due to impaired survival, proliferation, migration, recruitment, and differentiation of OPCs (Maki, et al., 2013). In the aging brain, there is white matter shrinkage and decreased myelination, which is exacerbated and accelerated in dementia, suggesting a decline in the regenerative capacity of OPCs (Rivera, et al., 2016). Our data show that MMI in RB rats significantly decreased the number of OPCs in the corpus callosum and striatum. These data indicate that MMI decreases myelin density as well as hinders remyelination of axons in the corpus callosum and striatal WM bundles.

4.3. MMI model induces axonal and synaptic damage in RB rats

Synaptic dysfunction contributes to AD dementia and is now gaining importance in mediating VaD (Clare, et al., 2010). Synaptophysin is the most abundant integral synaptic vesicle protein (Clare, et al., 2010), and our data indicate that there is a significant reduction in the expression levels of synaptophysin in the cortex and striatum of RB MMI rats. Dendritic spines which are actin rich protrusions from dendrites are a major contributor to synaptic plasticity. These spines enable synaptic transmission, increase contact points between neurons and play a key role in learning and memory (Yang, et al., 2009). Synapses, spines and synaptic plasticity are sites of memory storage (Okano, et al., 2000). Our results indicate a significant reduction in cortical neuronal branching and cortical and hippocampal spine density post MMI in RB rats.

4.4. MMI increases dilated perivascular spaces in RB rats

In dementias, vascular damage has been reported including increased BBB permeability, arterioles with a thickened vessel wall and perivascular dilatation with surrounding WM damage (Doubal, et al., 2010,Kril, et al., 2002). In the pathogenesis of dementia, failure to eliminate interstitial fluid (ISF) indicates a failure to clear soluble metabolic wastes which can lead to an imbalance of brain homeostasis (Weller, et al., 2015). Perivascular spaces enable lymphatic drainage of ISF from the brain, and the structure of these perivascular spaces are different around arteries and veins as well as different when in the cortex and basal ganglia (Pollock, et al., 1997). In dementia, while dilated perivascular spaces around arteries are not common in the cerebral cortex, in the WM and basal ganglia dilated perivascular spaces are present and thought to indicate an impaired solute and ISF clearance (Roher, et al., 2003,Weller, et al., 2015). Dilated perivascular spaces have been suggested as a valuable biomarker of small vessel disease among the elderly population (Hansen, et al., 2015) and may be due to glymphatic dysfunction (Wostyn, et al., 2016). In our study, we observed dilated perivascular spaces around arteries in the striatum that significantly correlate to WM damage. This suggests MMI may impair interstitial solute and waste clearance.

4.5. MMI decreases AQP-4 expression and induces glymphatic dysfunction in RB rats

Several recent studies have reported glymphatic dysfunction in neurological disease states such as stroke, and Alzheimer's disease (Jessen, et al., 2015). Reduction of AQP-4 post brain injury exacerbates glymphatic pathway dysfunction (J. J. Iliff, et al., 2014) and AQP-4 knockout mice exhibit slowed CSF influx via the glymphatic system and ~70% reduction in ISF solute clearance, giving a clear indication that the AQP-4 water channel mediates the glymphatic pathway (Iliff, et al., 2012). AQP-4 lined water channels provide low resistance pathways for fluid movement and exchange between the CSF in paravascular spaces and the ISF in parenchyma, linking paravascular and interstitial bulk flow, thereby facilitating waste clearance (Iliff, et al., 2012). Sudden decrease of AQP-4 occurs in regions of vascular damage after ischemia primarily to control the influx of water post injury (Friedman, et al., 2009). Age associated glymphatic dysfunction has been reported with decreased and delayed CSF penetration along paravascular pathways and pial surface (Kress, et al., 2014). Our data indicate decreased AQP-4 expression around blood vessels in RB rats subjected to MMI. AQP-4 expression around blood vessels significantly correlates to cognitive function. Our data also indicate an impairment of glymphatic function with delayed penetration and clearance of CSF via paravascular pathways; both ipsi- and contra-lateral CSF influx/efflux was affected. This is similar to previous reports of glymphatic dysfunction following AQP-4 loss in a traumatic brain injury model which also showed that both ipsi- and contra-lateral CSF influx was affected (Jeffrey J. Iliff, et al., 2014). Hence, it appears that water channel and glymphatic dysfunction, as indicated by dilated perivascular spaces, decreased AQP-4 expression and delayed penetration and clearance of tracers injected into the CSF, may play key roles in MMI induced VaD pathology.

4.6. Limitations

There are several limitations to this study. Firstly, while this model may be potentially clinically relevant and several studies have demonstrated that cholesterol crystal embolization can induce cognitive deficits, there are some differences in the observed infarctions (number, location and size) largely due to variations in the number and size of cholesterol crystals used (Rapp, et al., 2008a,Rapp, et al., 2008b,Wang, et al., 2012). Secondly, the MMI model appears to be highly sensitive to age as we have demonstrated as well as others (Rapp, et al., 2008b). Thirdly, the pathological events are time sensitive and this model primarily induces chronic inflammation and delayed axonal/white matter damage without inducing large infarctions. We have evaluated glymphatic function at only time point (2 weeks after MMI). Although there is a trend of AQP-4 recovery by 6 weeks after MMI, there is still significant damage to white matter as well as significant AQP-4 reduction (supplementary figure 6). Hence, we expect a similar trend for glymphatic dysfunction. We cannot rule out the possibility that glymphatic dysfunction is a result of several pathological events, including ischemic lesions and water channel dysfunction. Since we have shown an associative glymphatic dysfunction and have only assessed it at one time point in this study, it is difficult to discern the exact contributing factors. Underlying molecular mechanisms of MMI induced white matter and glymphatic damage are uncertain and further studies are warranted. Hypertension and diabetes are high risk factors for vascular dementia (Venkat, et al., 2015). Co-morbidity with diabetes or hypertension has been shown to aggravate stroke pathology and increase susceptibility to vascular and white matter damage upon ischemia

(Chen, et al., 2011,Wong and Read, 2008). This study has not investigated the effects of hypertension or diabetes after MMI and we speculate that MMI in RB rats with diabetes or hypertension would induce significant vascular and white matter damage and affect cognition. In this study, we have demonstrated multiple pathophysiological events induced by MMI in RB rats. We have demonstrated key correlations of pathophysiological events such as axonal/WM damage, water channel dysfunction and glymphatic dysfunction that may drive, independently or together, cognitive dysfunction. The underlying mechanisms of MMI induced multiple pathophysiological events and how these events couple and possibly act in concert to produce VaD has not been investigated in the present study and future studies are warranted.

5. Conclusions

In this study, we show that an MMI model age dependently induces VaD, and RB rats are most suitable for establishing an MMI based VaD model. The MMI-RB model induces cognitive deficits, and axonal/WM damage which persist at least until 6 weeks after MMI. Decreasing AQP-4, increasing perivascular space and glymphatic dysfunction are associated with and may drive axonal/WM damage and cognitive deficit. Therefore, the glymphatic system pathway and axonal/WM damage may be targets for VaD therapy.

Supplementary Material

Refer to Web version on PubMed Central for supplementary material.

Acknowledgements

The authors wish to thank Qinge Lu and Sutapa Santra for the technical assistance and Amy Kemper for help with sample preparation and acquisition of electron microscopy images.

Sources of Funding: This work was supported by National Institute of Neurological Disorders and Stroke RO1 NS083078 (J.C.), R01NS099030 (J.C), RO1 NS088656 (M.C.).

Abbreviations

AQP-4	Aquaporin-4
BBB	Blood brain barrier
BS	Bielschowsky silver
CCA	Common carotid artery
CSF	Cerebrospinal fluid
ECA	External carotid artery
EM	Electron microscopy
ICA	Internal carotid artery
ISF	Interstitial fluid

LFB	Luxol fast blue
MMI	Multiple microinfarction
mNSS	Modified nuerological severity score
OL	Oligodendrocyte
OPC	Oligodendrocyte progenitor cells
RB	Retired breeder
VaD	Vascular dementia
WM	White matter

References

Ampawong S, Combes V, Hunt NH, Radford J, Chan-Ling T, Pongponratn E, Grau GER. Quantitation of brain edema and localisation of aquaporin 4 expression in relation to susceptibility to experimental cerebral malaria. International journal of clinical and experimental pathology. 2011; 4(6):566–74. [PubMed: 21904632]

Badaut J, Ashwal S, Obenaus A. Aquaporins in cerebrovascular disease: a target for treatment of brain edema? Cerebrovasc Dis. 2011; 31(6):521–31. doi:10.1159/000324328. [PubMed: 21487216]

Brown R, Corey S, Moore A. Differences in Measures of Exploration and Fear in MHC-Congenic C57BL/6J and B6-H-2K Mice. Behav Genet. 1999; 29(4):263–71. doi:10.1023/a:1021694307672.

Chen J, Cui X, Zacharek A, Cui Y, Roberts C, Chopp M. White matter damage and the effect of matrix metalloproteinases in type 2 diabetic mice after stroke. Stroke. 2011; 42(2):445–52. doi:10.1161/STROKEAHA.110.596486. [PubMed: 21193743]

Chen J, Li Y, Wang L, Zhang Z, Lu D, Lu M, Chopp M. Therapeutic benefit of intravenous administration of bone marrow stromal cells after cerebral ischemia in rats. Stroke. 2001; 32(4): 1005–11. [PubMed: 11283404]

Chen J, Ning R, Zacharek A, Cui C, Cui X, Yan T, Venkat P, Zhang Y, Chopp M. MiR-126 Contributes to Human Umbilical Cord Blood Cell-Induced Neurorestorative Effects After Stroke in Type-2 Diabetic Mice. Stem cells (Dayton, Ohio). 2016; 34(1):102–13. doi:10.1002/stem.2193.

Chida Y, Kokubo Y, Sato S, Kuge A, Takemura S, Kondo R, Kayama T. The alterations of oligodendrocyte, myelin in corpus callosum, and cognitive dysfunction following chronic cerebral ischemia in rats. Brain Res. 2011; 1414:22–31. doi:10.1016/j.brainres.2011.07.026. [PubMed: 21864831]

Clare R, King VG, Wirenfeldt M, Vinters HV. Synapse loss in dementias. J Neurosci Res. 2010; 88(10):2083–90. doi:10.1002/jnr.22392. [PubMed: 20533377]

Darwish H, Mahmood A, Schallert T, Chopp M, Therrien B. Mild traumatic brain injury (MTBI) leads to spatial learning deficits. Brain injury. 2012; 26(2):151–65. doi:10.3109/02699052.2011.635362. [PubMed: 22360521]

Doubal FN, MacLullich AM, Ferguson KJ, Dennis MS, Wardlaw JM. Enlarged perivascular spaces on MRI are a feature of cerebral small vessel disease. Stroke. 2010; 41(3):450–4. doi:10.1161/STROKEAHA.109.564914. [PubMed: 20056930]

Erkinjuntti T, Benavente O, Eliasziw M, Munoz DG, Sulkava R, Haltia M, Hachinski V. Diffuse vacuolization (spongiosis) and arteriolosclerosis in the frontal white matter occurs in vascular dementia. Archives of neurology. 1996; 53(4):325–32. [PubMed: 8929154]

Fields RD. White matter in learning, cognition and psychiatric disorders. Trends in neurosciences. 2008; 31(7):361–70. doi:10.1016/j.tins.2008.04.001. [PubMed: 18538868]

Friedman B, Schachtrup C, Tsai PS, Shih AY, Akassoglou K, Kleinfeld D, Lyden PD. Acute vascular disruption and aquaporin 4 loss after stroke. Stroke. 2009; 40(6):2182–90. doi:10.1161/strokeaha.108.523720. [PubMed: 19372455]

Hansen TP, Cain J, Thomas O, Jackson A. Dilated perivascular spaces in the Basal Ganglia are a biomarker of small-vessel disease in a very elderly population with dementia. AJNR American journal of neuroradiology. 2015; 36(5):893–8. doi:10.3174/ajnr.A4237. [PubMed: 25698626]

Iliff JJ, Chen MJ, Plog BA, Zeppenfeld DM, Soltero M, Yang L, Singh I, Deane R, Nedergaard M. Impairment of glymphatic pathway function promotes tau pathology after traumatic brain injury. The Journal of neuroscience : the official journal of the Society for Neuroscience. 2014; 34(49): 16180–93. doi:10.1523/jneurosci.3020-14.2014. [PubMed: 25471560]

Iliff JJ, Chen MJ, Plog BA, Zeppenfeld DM, Soltero M, Yang L, Singh I, Deane R, Nedergaard M. Impairment of Glymphatic Pathway Function Promotes Tau Pathology after Traumatic Brain Injury. The Journal of Neuroscience. 2014; 34(49):16180–93. doi:10.1523/JNEUROSCI. 3020-14.2014. [PubMed: 25471560]

Iliff JJ, Wang M, Liao Y, Plogg BA, Peng W, Gundersen GA, Benveniste H, Vates GE, Deane R, Goldman SA, Nagelhus EA, Nedergaard M. A paravascular pathway facilitates CSF flow through the brain parenchyma and the clearance of interstitial solutes, including amyloid beta. Sci Transl Med. 2012; 4(147):147ra11. doi:10.1126/scitranslmed.3003748.

Ishii N, Nishihara Y, Imamura T. Why do frontal lobe symptoms predominate in vascular dementia with lacunes? Neurology. 1986; 36(3):340–5. [PubMed: 3951700]

Jessen NA, Munk AS, Lundgaard I, Nedergaard M. The Glymphatic System: A Beginner's Guide. Neurochemical research. 2015; 40(12):2583–99. doi:10.1007/s11064-015-1581-6. [PubMed: 25947369]

Jiang Q, Zhang L, Ding G, Davoodi-Bojd E, Li Q, Li L, Sadry N, Nedergaard M, Chopp M, Zhang Z. Impairment of the glymphatic system after diabetes. J Cereb Blood Flow Metab. 2016 doi: 10.1177/0271678X16654702.

Kress BT, Iliff JJ, Xia M, Wang M, Wei HS, Zeppenfeld D, Xie L, Kang H, Xu Q, Liew JA, Plog BA, Ding F, Deane R, Nedergaard M. Impairment of paravascular clearance pathways in the aging brain. Ann Neurol. 2014; 76(6):845–61. doi:10.1002/ana.24271. [PubMed: 25204284]

Kril JJ, Patel S, Harding AJ, Halliday GM. Patients with vascular dementia due to microvascular pathology have significant hippocampal neuronal loss. Journal of Neurology, Neurosurgery & Psychiatry. 2002; 72(6):747–51. doi:10.1136/jnnp.72.6.747.

Laloux P, Brucher JM. Lacunar infarctions due to cholesterol emboli. Stroke. 1991; 22(11):1440–4. [PubMed: 1750055]

Maki T, Liang AC, Miyamoto N, Lo EH, Arai K. Mechanisms of oligodendrocyte regeneration from ventricular-subventricular zone-derived progenitor cells in white matter diseases. Frontiers in Cellular Neuroscience. 2013; 7:275. doi:10.3389/fncel.2013.00275. [PubMed: 24421755]

Merluzzi AP, Dean DC 3rd, Adluru N, Suryawanshi GS, Okonkwo OC, Oh JM, Hermann BP, Sager MA, Asthana S, Zhang H, Johnson SC, Alexander AL, Bendlin BB. Age-dependent differences in brain tissue microstructure assessed with neurite orientation dispersion and density imaging. Neurobiol Aging. 2016; 43:79–88. doi:10.1016/j.neurobiolaging.2016.03.026. [PubMed: 27255817]

Okano H, Hirano T, Balaban E. Learning and memory. Proceedings of the National Academy of Sciences. 2000; 97(23):12403–4. doi:10.1073/pnas.210381897.

Papadopoulos MC, Krishna S, Verkman AS. Aquaporin water channels and brain edema. The Mount Sinai journal of medicine, New York. 2002; 69(4):242–8.

Plassman BL, Langa KM, Fisher GG, Heeringa SG, Weir DR, Ofstedal MB, Burke JR, Hurd MD, Potter GG, Rodgers WL, Steffens DC, Willis RJ, Wallace RB. Prevalence of dementia in the United States: the aging, demographics, and memory study. Neuroepidemiology. 2007; 29(1-2): 125–32. doi:10.1159/000109998. [PubMed: 17975326]

Pollock H, Hutchings M, Weller RO, Zhang ET. Perivascular spaces in the basal ganglia of the human brain: their relationship to lacunes. Journal of anatomy. 1997; 191(Pt 3):337–46. [PubMed: 9418990]

Prakash R, Li W, Qu Z, Johnson MA, Fagan SC, Ergul A. Vascularization pattern after ischemic stroke is different in control versus diabetic rats: relevance to stroke recovery. Stroke. 2013; 44(10):2875–82. doi:10.1161/strokeaha.113.001660. [PubMed: 23920018]

Rapp JH, Hollenbeck K, Pan XM. An experimental model of lacunar infarction: embolization of microthrombi. Journal of vascular surgery. 2008a; 48(1):196–200. doi:10.1016/j.jvs.2008.01.038. [PubMed: 18486421]

Rapp JH, Pan XM, Neumann M, Hong M, Hollenbeck K, Liu J. Microemboli composed of cholesterol crystals disrupt the blood-brain barrier and reduce cognition. Stroke. 2008b; 39(8):2354–61. doi: 10.1161/strokeaha.107.496737. [PubMed: 18566307]

Rennels ML, Gregory TF, Blaumanis OR, Fujimoto K, Grady PA. Evidence for a 'paravascular' fluid circulation in the mammalian central nervous system, provided by the rapid distribution of tracer protein throughout the brain from the subarachnoid space. Brain Res. 1985; 326(1):47–63. [PubMed: 3971148]

Rivera A, Vanzuli I, Arellano JJ, Butt A. Decreased Regenerative Capacity of Oligodendrocyte Progenitor Cells (NG2-Glia) in the Ageing Brain: A Vicious Cycle of Synaptic Dysfunction, Myelin Loss and Neuronal Disruption? Curr Alzheimer Res. 2016; 13(4):413–8. [PubMed: 26567743]

Roher AE, Kuo YM, Esh C, Knebel C, Weiss N, Kalback W, Luehrs DC, Childress JL, Beach TG, Weller RO, Kokjohn TA. Cortical and leptomeningeal cerebrovascular amyloid and white matter pathology in Alzheimer's disease. Molecular medicine. 2003; 9(3-4):112–22. [PubMed: 12865947]

Spinetta MJ, Woodlee MT, Feinberg LM, Stroud C, Schallert K, Cormack LK, Schallert T. Alcohol-induced retrograde memory impairment in rats: prevention by caffeine. Psychopharmacology (Berl). 2008; 201(3):361–71. doi:10.1007/s00213-008-1294-5. [PubMed: 18758756]

Steiner TJ, Rail DL, Rose FC. Cholesterol crystal embolization in rat brain: a model for atheroembolic cerebral infarction. Stroke. 1980; 11(2):184–9. [PubMed: 7368248]

Stuart SA, Robertson JD, Marrion NV, Robinson ES. Chronic pravastatin but not atorvastatin treatment impairs cognitive function in two rodent models of learning and memory. PloS one. 2013; 8(9):e75467. doi:10.1371/journal.pone.0075467. [PubMed: 24040413]

Sultzer DL, Mahler ME, Cummings JL, Van Gorp WG, Hinkin CH, Brown C. Cortical abnormalities associated with subcortical lesions in vascular dementia. Clinical and position emission tomographic findings. Archives of neurology. 1995; 52(8):773–80. [PubMed: 7639629]

Tanabe JL, Ezekiel F, Jagust WJ, Reed BR, Norman D, Schuff N, Weiner MW, Chui H, Fein G. Magnetization transfer ratio of white matter hyperintensities in subcortical ischemic vascular dementia. AJNR American journal of neuroradiology. 1999; 20(5):839–44. [PubMed: 10369354]

Tokuchi R, Hishikawa N, Sato K, Hatanaka N, Fukui Y, Takemoto M, Ohta Y, Yamashita T, Abe K. Age-dependent cognitive and affective differences in Alzheimer's and Parkinson's diseases in relation to MRI findings. J Neurol Sci. 2016; 365:3–8. doi:10.1016/j.jns.2016.03.031. [PubMed: 27206864]

Venkat P, Chopp M, Chen J. Models and mechanisms of vascular dementia. Exp Neurol. 2015 doi: 10.1016/j.expneurol.2015.05.006.

Wang M, Iliff JJ, Liao Y, Chen MJ, Shinseki MS, Venkataraman A, Cheung J, Wang W, Nedergaard M. Cognitive deficits and delayed neuronal loss in a mouse model of multiple microinfarcts. The Journal of neuroscience : the official journal of the Society for Neuroscience. 2012; 32(50):17948–60. doi:10.1523/JNEUROSCI.1860-12.2012. [PubMed: 23238711]

Weller RO, Hawkes CA, Kalaria RN, Werring DJ, Carare RO. White matter changes in dementia: role of impaired drainage of interstitial fluid. Brain pathology. 2015; 25(1):63–78. doi:10.1111/bpa.12218. [PubMed: 25521178]

Wong AA, Read SJ. Early changes in physiological variables after stroke. Annals of Indian Academy of Neurology. 2008; 11(4):207–20. doi:10.4103/0972-2327.44555. [PubMed: 19893676]

Wostyn P, De Groot V, Van Dam D, Audenaert K, Killer HE, De Deyn PP. Dilated Virchow-Robin spaces in primary open-angle glaucoma: a biomarker of glymphatic waste clearance dysfunction? Acta Radiol Open. 2016; 5(8):2058460116653630. doi:10.1177/2058460116653630. [PubMed: 27570637]

Yan T, Venkat P, Chopp M, Zacharek A, Ning R, Cui Y, Roberts C, Kuzmin-Nichols N, Sanberg CD, Chen J. Neurorestorative Therapy of Stroke in Type 2 Diabetes Mellitus Rats Treated With Human Umbilical Cord Blood Cells. Stroke. 2015 doi:10.1161/strokeaha.115.009870.

Yan T, Venkat P, Ye X, Chopp M, Zacharek A, Ning R, Cui Y, Roberts C, Kuzmin-Nichols N, Sanberg CD, Chen J. HUCBCs Increase Angiopoietin 1 and Induce Neurorestorative Effects after Stroke in T1DM Rats. CNS neuroscience & therapeutics. 2014; 20(10):935–44. doi:10.1111/cns.12307. [PubMed: 25042092]

Yang G, Pan F, Gan WB. Stably maintained dendritic spines are associated with lifelong memories. Nature. 2009; 462(7275):920–4. doi:10.1038/nature08577. [PubMed: 19946265]

Yang L, Kress BT, Weber HJ, Thiyagarajan M, Wang B, Deane R, Benveniste H, Iliff JJ, Nedergaard M. Evaluating glymphatic pathway function utilizing clinically relevant intrathecal infusion of CSF tracer. J Transl Med. 2013; 11:107. doi:10.1186/1479-5876-11-107. [PubMed: 23635358]

Zhang R, Chopp M, Zhang ZG. Oligodendrogenesis after cerebral ischemia. Frontiers in Cellular Neuroscience. 2013; 7:201. doi:10.3389/fncel.2013.00201. [PubMed: 24194700]

Zhang ZG, Zhang L, Jiang Q, Zhang R, Davies K, Powers C, Bruggen N.v. Chopp M. VEGF enhances angiogenesis and promotes blood-brain barrier leakage in the ischemic brain. Journal of Clinical Investigation. 2000; 106(7):829–38. [PubMed: 11018070]

Highlights

- Multiple Microinfarction (MMI) in retired breeder (RB) rats impairs cognition
- MMI in RB rats, damages white matter and synaptic plasticity
- MMI in RB rats, impairs water channel and glymphatic function

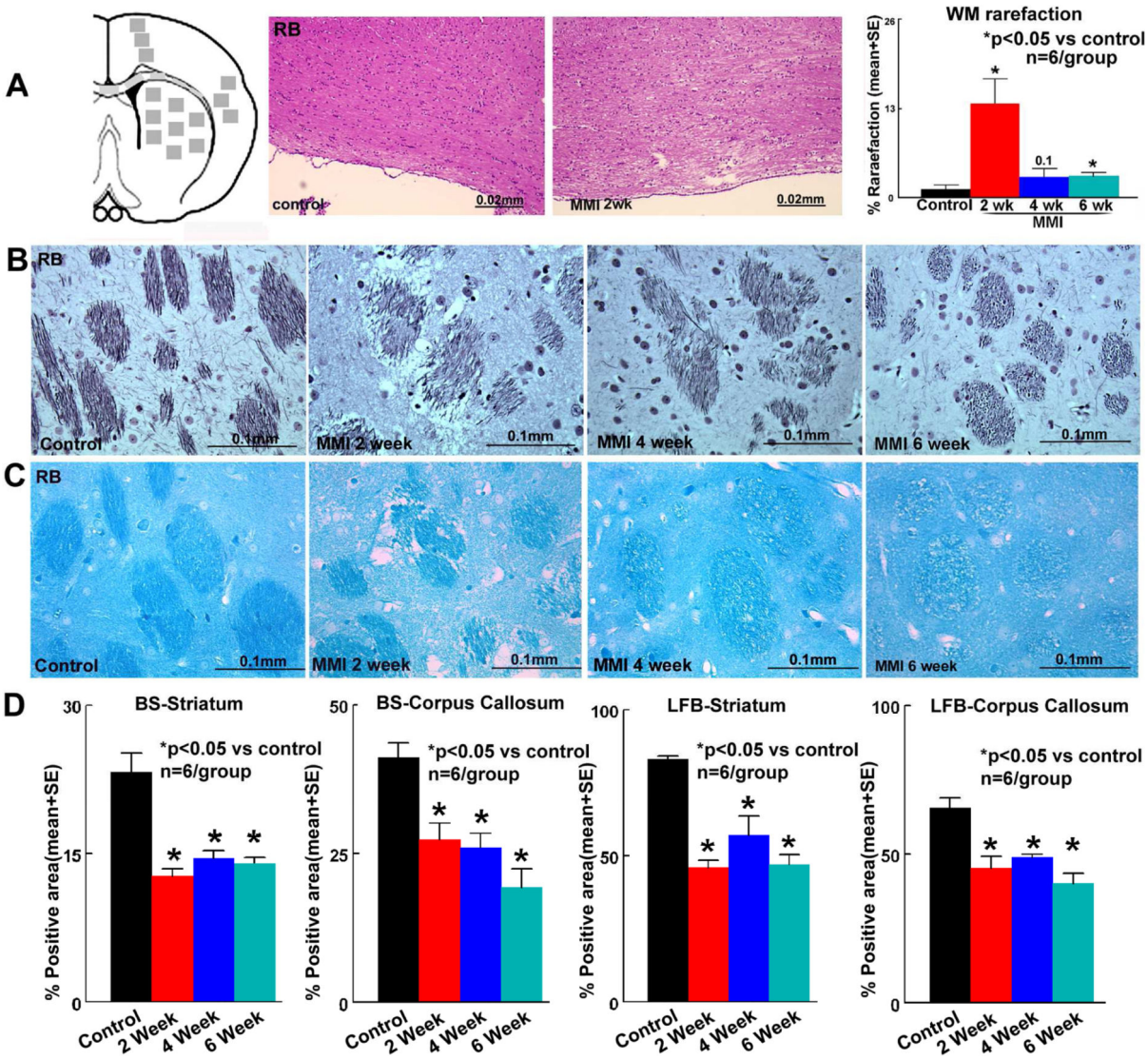

Figure 1. MMI induces significant axonal/WM damage in RB rats

A) Schematic of immunohistochemical quantification areas; MMI in RB rats induces significant WM rarefaction early after MMI. MMI in RB rats induces significant B) axon damage-Bielschowsky silver staining and C) myelin damage-Luxol fast blue in corpus callosum and striatum WM bundles compared to RB control rats which persists until 6 weeks after MMI; D) quantification data.

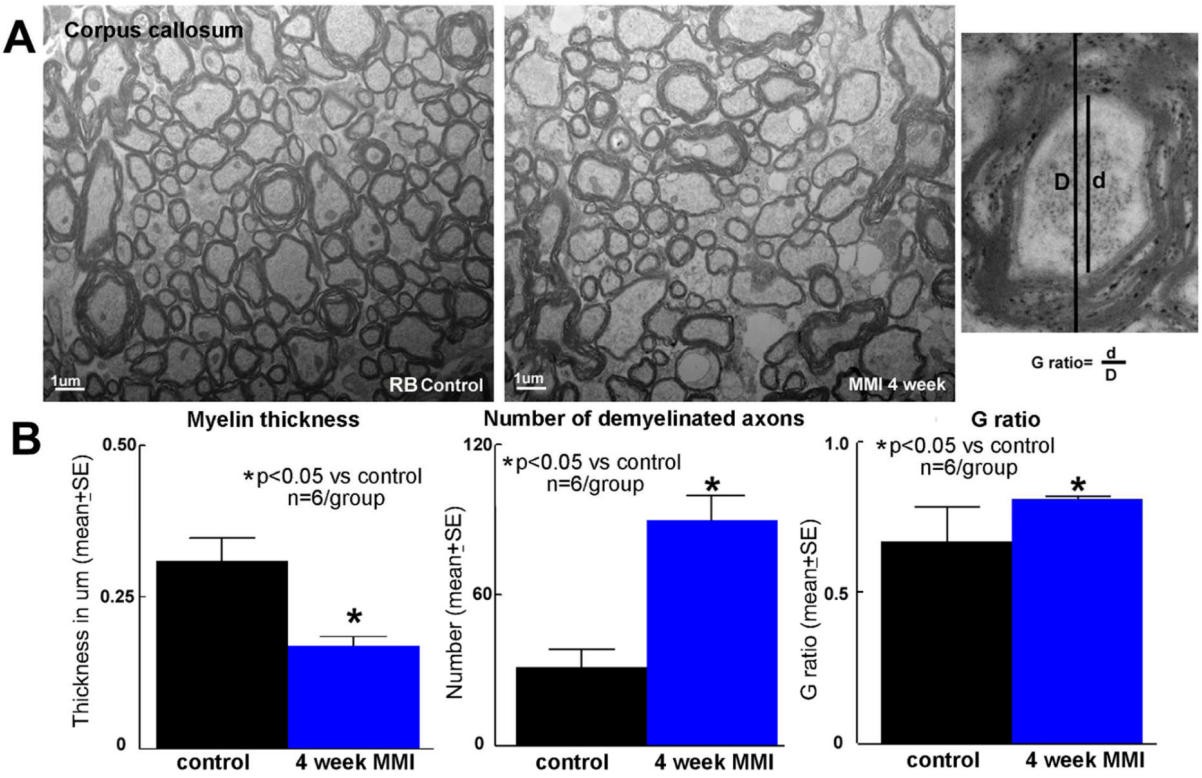

Figure 2. Electron microscopy-MMI induces significant axonal/WM damage in RB rats

A) MMI in RB rats induces significantly decrease in myelin thickness, increases number of demyelinated axons and G ratio in the corpus callosum compared to control RB rats; B) quantification data.

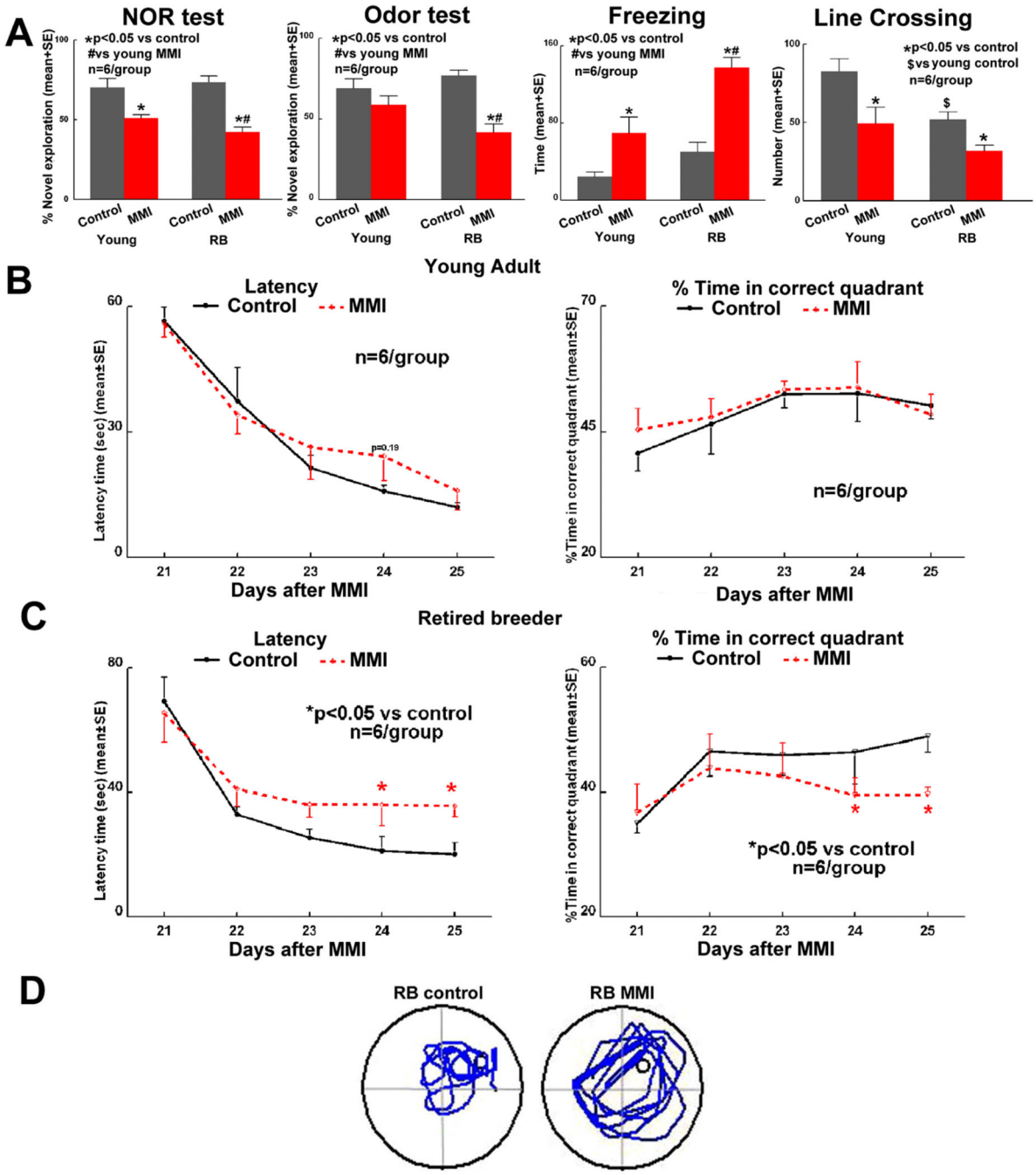

Figure 3. MMI induces cognitive deficits which worsen with increasing age

MMI induces memory loss which worsens with age compared to age-matched controls. A) Short term memory-Novel object recognition test; long-term memory-Odor test; anxiety-like behavior and exploratory activity-Open field test. B-D) MMI in RB rats and not young rats induces significant spatial learning and memory deficits.

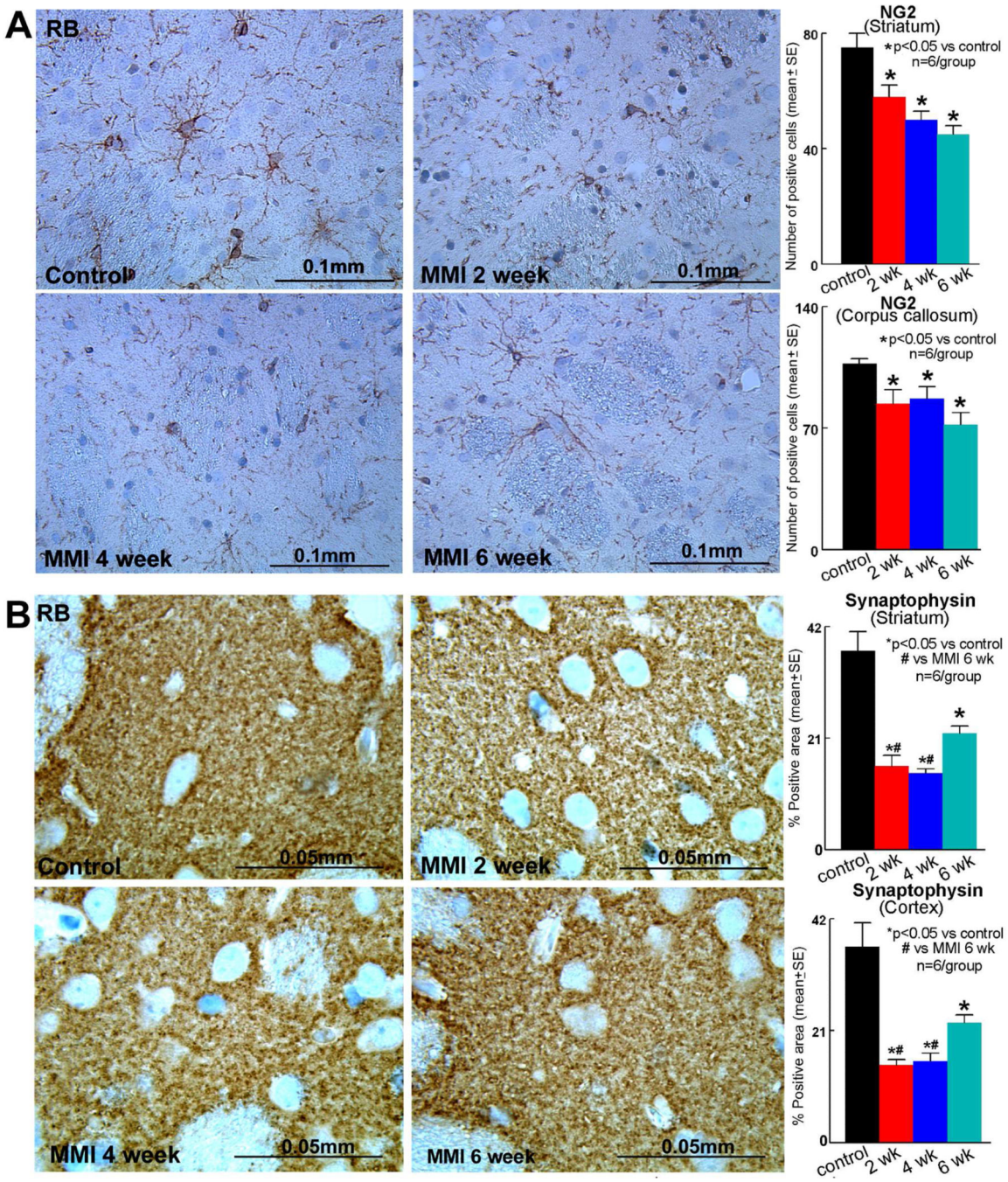

Figure 4. MMI decreases OPCs and synaptophysin expression in RB rats

Compared to RB control rats, MMI in RB rats significantly decreases A) oligodendrocytes progenitor cell numbers in the corpus callosum and striatum (NG2 staining); B) synaptic protein expression (Synaptophysin) in the cortex and striatum, which persist until 6 weeks after MMI.

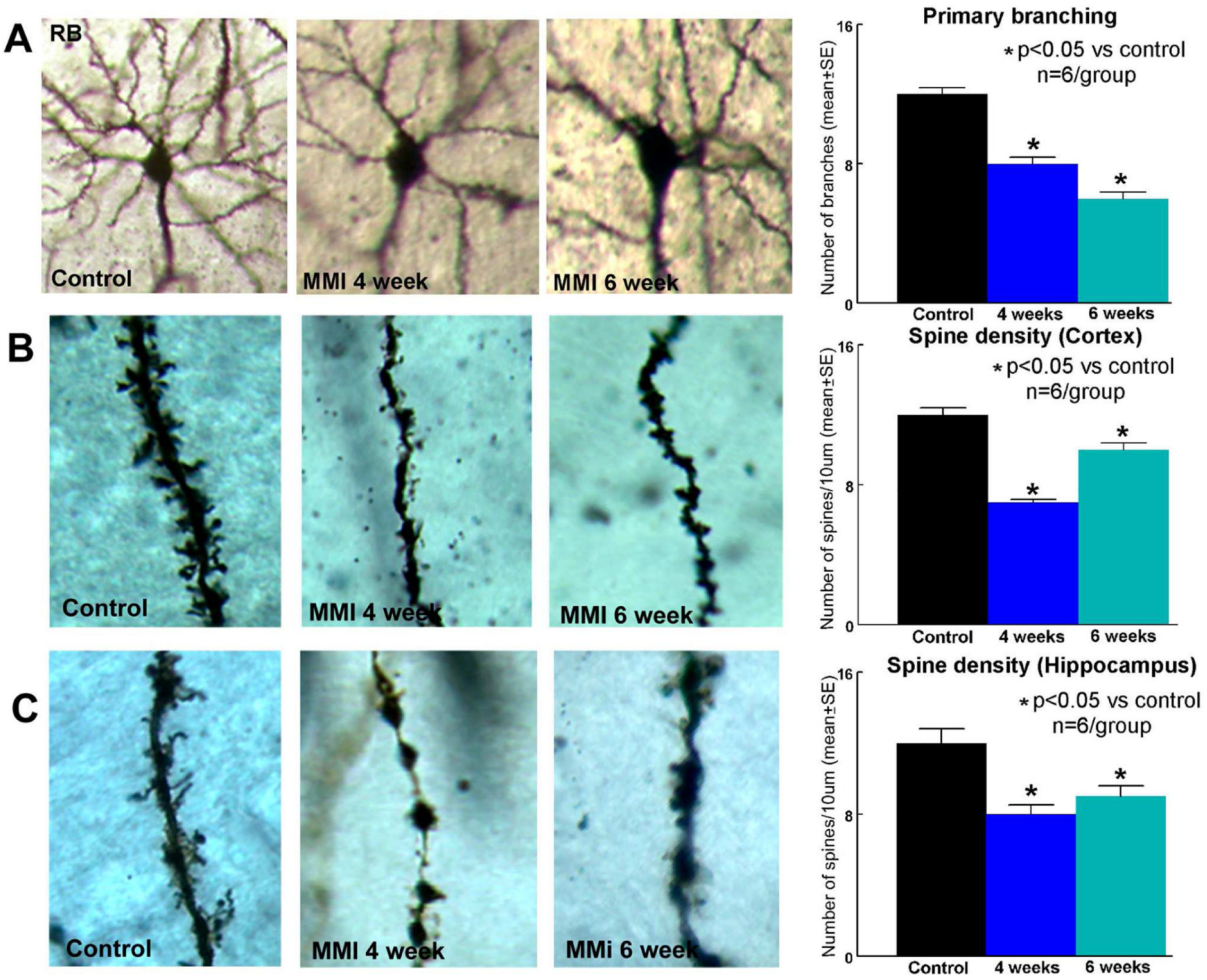

Figure 5. Golgi Staining

A) MMI in RB rats significantly decreases cortical neuronal branching and decreases B) cortical and C) hippocampal spine density compared to RB control rats which persists until 6 weeks after MMI.

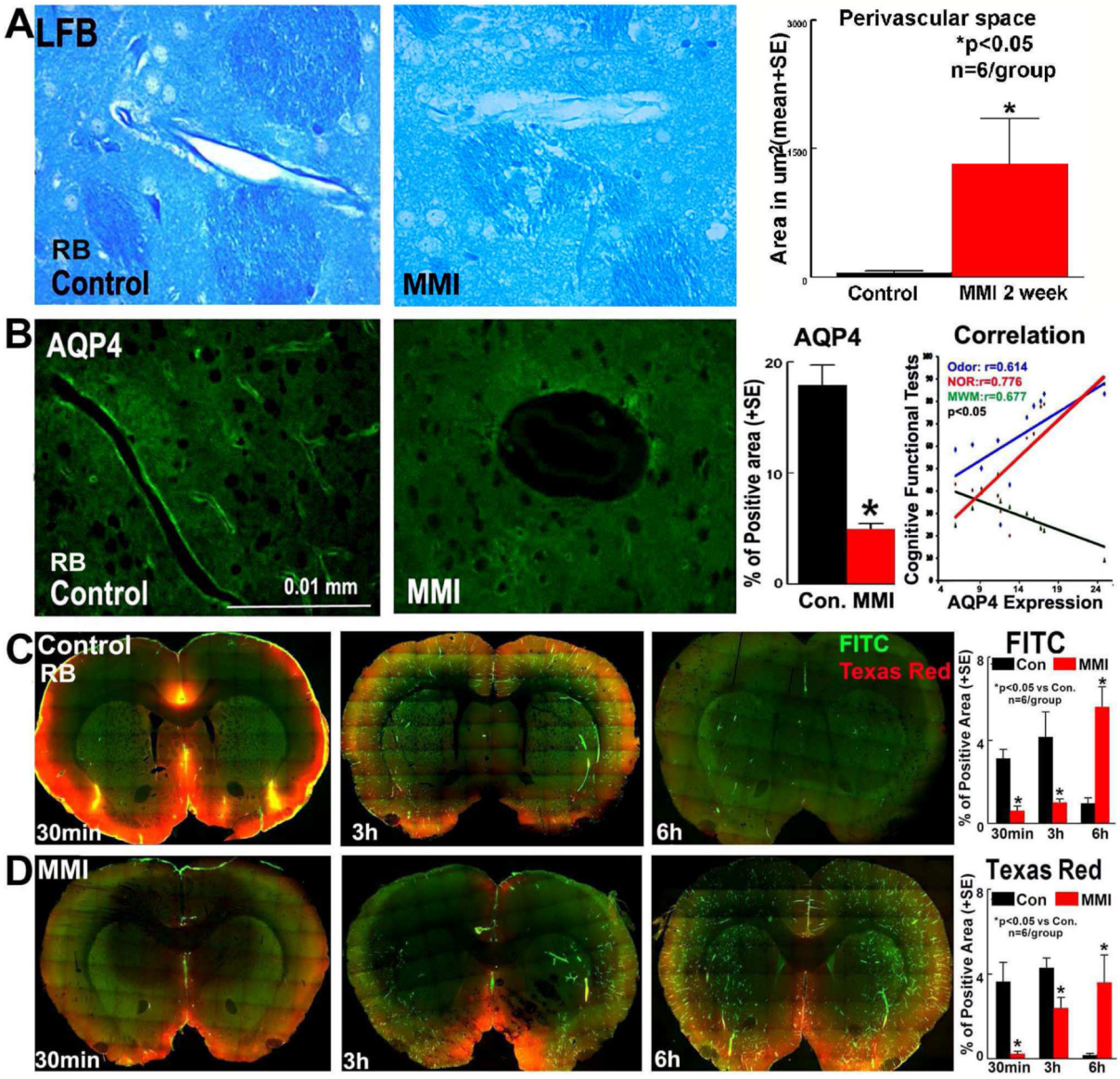

Figure 6. MMI in RB rats induces water channel and glymphatic dysfunction

A) MMI in RB rats induces dilated perivascular spaces. B) MMI in RB rats significantly decreases AQP-4 expression around blood vessels in the brain and this water channel dysfunction persists until 6 weeks after MMI. AQP-4 loss is significantly correlated with cognitive dysfunction. C-D) MMI in RB rats significantly induces a delay in CSF penetration and clearance via paravascular pathways.